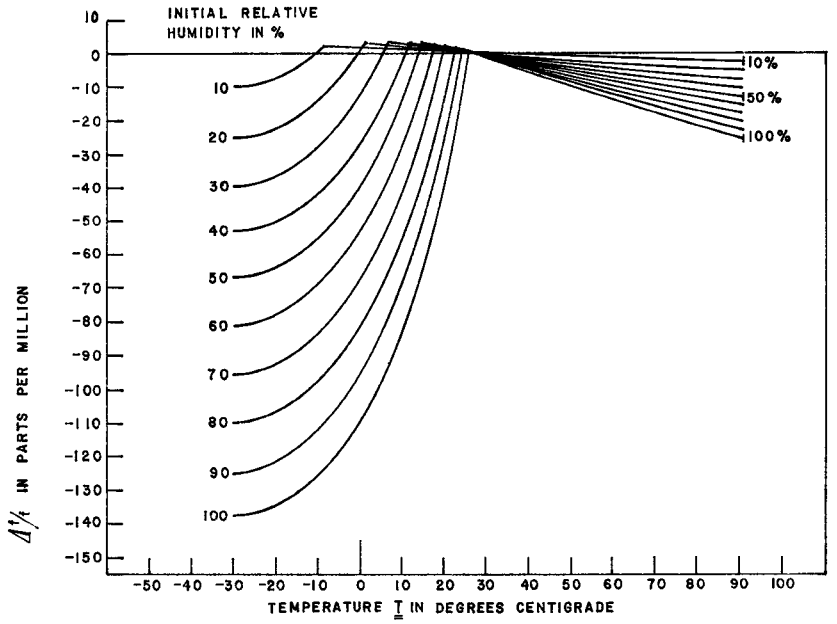

Fig. 3. Frequency shift as a function of temperature for a cavity sealed at 25°C for several different initial relative humidities. Curves apply to a closed system only. Values are to be added to measured values.

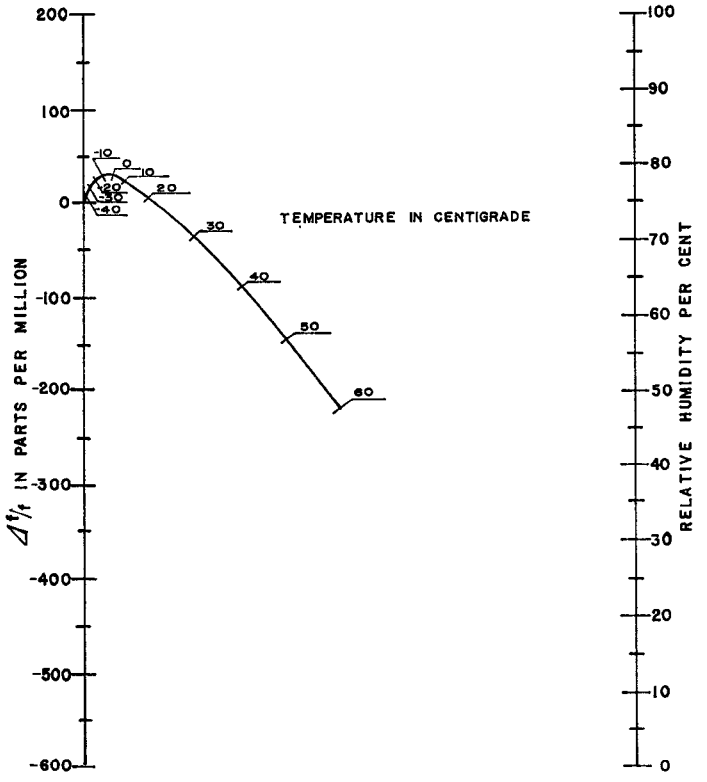

Fig. 4. Nomograph for computing frequency shift as a function of temperature and humidity for an open cavity. $\Delta f/f$ values are read from the intersection of the $\Delta f/f$ scale and the line which joins temperature with relative humidity. Nomograph values are to be added to measured values. (After Montgomery.)

closed system, then all calculations in (2) and (4) must be carried out for these conditions.

Let us now compare the results of Montgomery's nomograph, shown in Fig. 4, to those obtained for the closed system. For both cases let the initial condition of the cavity be 60 percent relative humidity at 25°C and 1 atmosphere. Assume that the frequency shift is desired for the case in which the final temperature is −5°C and the relative humidity is 100 percent. Considering the closed system first, it is obvious that the initial conditions are satisfied by the 60 percent line of Fig. 3. Since the sealed cavity forms a closed system, the same line will satisfy the final conditions of 100 percent relative humidity at −5°C.

From Fig. 3 we see that the frequency shift is plus 62 PPM (since values on the graph are to be added to measured values). Entering the nomograph of Fig. 4 we see that the predicted frequency shift is minus 30 PPM. The reason for the difference in values is due to the fact that the dielectric constant changes minus 90 PPM due to the change of the mass of dry air, and plus 60 PPM for the water vapor in the open system, resulting in a net shift of minus 30 PPM.

It should be pointed out that in actual laboratory measurements there are many other errors to be accounted for. For example, it is well known that water vapor causes an increased absorption level in the K band and that these losses will cause a frequency shift. In addition, at lower temperatures, water precipitation on resonator walls will cause a frequency shift which must be handled with perturbation techniques. The thermal expansion of the cavity walls must also be accounted for.

Actually, for resonators built from conventional materials (aluminum, brass, etc.), the error due to thermal expansion of the walls far exceeds the error introduced by humidity effects. Recently developed resonators built from low-expansion glass ceramics, however, exhibit thermal stabilities of several parts in 10^8. In such resonators, the humidity effect can far overshadow the thermal expansion of the walls.

Still another problem which must be dealt with is the differential of pressure from inside to outside of the resonator which causes mechanical deformation.[8] All of these factors as well as several other minor ones have made it very difficult to precisely confirm the above analysis experimentally. Nevertheless, sufficient work has been performed to indicate that the above treatment is correct.

D. M. Smith
Corning Glass Works
Raleigh, N. C.

[8] C. M. Crain and C. E. Williams, "Method of obtaining pressure and temperature insensitive microwave cavity resonators," *Rev. Sci. Instr.*, vol. 28, pp. 620–623, August 1957.

Optimum Elliptic-Function Filters for Distributed Constant Systems

***Abstract*—It is shown from an example that the derivation of distributed constant filters from lumped-element filters through Kuroda's transformation leads to less selectivity than can be obtained with the same number of elements, when the unit elements are also made to contribute to the filtering.**

Manuscript received January 5, 1967; revised March 27, 1967.

In a recent paper,[1] design tables for a wideband elliptic-function bandstop transmission-line filter have been described. The method of computation starts from a lumped-element (LE) filter specified in the catalogue of Saal. Several unit elements (UE), with unit normalized characteristic impedance, are put in cascade with this LE filter. By a succession of Kuroda's transformations, these UE are shifted within the LE 2-port, in order to yield a structure convenient for implementation with transmission lines (TL).

The UE in cascade constitute an all-pass 2-port. Hence the original LE filter and the resulting TL filter have the same attenuation characteristic. Although the latter is undoubtedly elliptic, it does not offer the optimum selectivity attainable with the same element cost, because the filtering ability of the UE in cascade is not made use of when their characteristic impedances are restricted to unity. An improved design lifts this restriction and optimizes directly the TL filter characteristic.

Consider the filter given in Fig. 3 of Schiffmann and Young.[1] Let $H(p)=f(p)/g(p)$ be the transmittance of a 2-port, where $f(p)$ and $g(p)$ are polynomials of degree n and m, respectively. For the filter of Fig. 3,[1] $n=4$ and $m=5$. Adding a cascade of four UE yields the filter of Fig. 5[1] with $n=8$ and $m=9$. With this value of m it is possible to locate nine attenuation zeros in the passband instead of the five attenuation zeros provided by the design of Schiffmann and Young.[1]

The approximation process can be made according to the theoretical approach of Ozaki and Ishii[2] or can be realized by a computer program yielding a Chebyshev behavior in both passband and stopband. The only particularity is the compulsory location of two double roots of f at ± 1. The two other pairs of roots of f are located in order to maximize the minimum of attenuation in the stopband. Simultaneously the nine attenuation zeros are selected to minimize the maximum of attenuation in the passband.

This process has been applied to the "trial" filter described in Schiffmann and Young.[1] With all other factors kept constant (0.28 dB of ripple in the band or 0.25 maximum reflection coefficient, selectivity specified by bandwidth ratios 1 and 0.34), the stopband attenuation obtained is 64.9 dB compared to 41.2 dB in Schiffmann and Young,[1] a discrimination increase of 23.7 dB. The curves are compared in Fig. 1. There is a small difference in the ripple (less than 0.02 dB) due to rounding-off errors.

It is interesting to observe that the attenuation ratio (64.9/41.2) is surprisingly close to the ratio of effective filtering components (11/7). This points to the fact that the filtering potential of the UE in cascade equals that of the UE in the stubs. Neglecting this potential amounts to a proportional lack in selectivity.

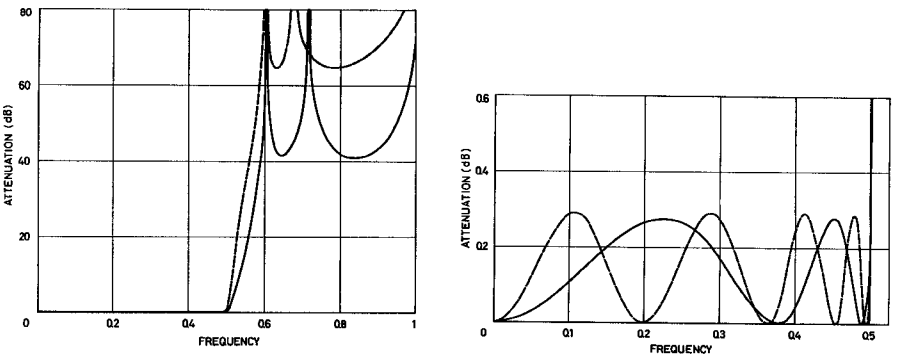

Fig. 1. (a) Attenuation of the Schiffmann and Young filter (solid line) compared to the attenuation of the optimum filter (dotted line). The frequency axis refers to the imaginary part of the dimensionless complex variable obtained through Richards' mapping. (b) Detail of the passband attenuation. The optimum filter presents one attenuation zero at the origin and four pairs of attenuation zeros versus two pairs for the Schiffmann and Young filter.

From other designs, it appears that the proportionality of the discrimination to the number of effective filtering components is a general rule. This can be justified on the basis of an image parameter theory. Although the actual designs are made on an effective behavior basis, it is well known that the image parameter theory gives a good estimate of the global performances. To take care of the UE in cascade, Soldi[3] has introduced the concept of the $\frac{1}{2}K\psi$ section. This section has an image attenuation which is formally the same as that of a m-derived, lumped parameter half section, with a value of m larger than unity, contrary to the common m-derived section. Nevertheless, this section brings a substantial amount of attenuation in the stopband. As far as the sections, with different m values, produce discriminations of the same order of magnitude, the total discrimination is proportional to the number of effective filtering sections.

The new design has been synthesized with the same structure as represented in Fig. 1 of Schiffmann and Young.[1] The values of the elements, labeled with the same notations, are

$$Z_1 = 0.6837 \qquad Z_{34} = 1.553$$
$$Z_{12} = 1.535 \qquad Z_4' = 0.9972$$
$$Z_2' = 0.6919 \qquad Z_4'' = 1.884$$
$$Z_2'' = 2.135 \qquad Z_{45} = 1.416$$
$$Z_{23} = 1.659 \qquad Z_5 = 0.7103.$$
$$Z_3 = 0.4231$$

As a bonus, the improved design method has also restricted the range of characteristic impedances to $2.135/0.4231 = 5.05$ compared to $5.147/0.445 = 11.6$ in Schiffmann and Young.[1]

To summarize, the solution obtained here presents some significant improvements with respect to that obtained in Schiffmann and Young.[1] The importance of the UE in tandem was emphasized in Ozaki and Ishii:[2] the last example given[2] meets similar attenuation requirements as the trial filter[1] with five UE instead of nine. An optimum design relies on a slightly more sophisticated method which requires a computer. As the number of UE in tandem lies between one third and one half of the total number of elements, their filtering capability should be utilized whenever a computer is available.

L. Fraiture
J. Neirynck
MBLE Research Lab.
Brussels, Belgium

Higher Order Modes in Rectangular Coaxial Waveguides

A precise determination of the characteristic impedance of rectangular coaxial waveguides has been recently undertaken by Cruzan and Garver [1] and it is well known that these structures have many applications in the design of shielded striplines, varactor mounts, etc. While their operation is, in general, confined to the TEM mode, there are instances when higher-order modes must be taken into account; the effect of the latter on striplines has been studied by Oliner [2], but there appears to be no record of a similar investigation applicable to rectangular coaxial waveguides.

In what follows, a symmetrical structure will be considered, i.e., the centers of the inner and outer conductors will be assumed to coincide. Furthermore, reference will be made to TE_{nm} and TM_{nm} modes to conform with standard notation for single-ridge waveguides [3] as well as rectangular waveguides.

Inspection of Fig. 1 shows that when the subscripts m or n or both are even, the planes of symmetry MN or KL or both are electric walls and the field pattern may be deduced from that of the corresponding single-ridge waveguide. On the other hand, the $TE_{2n+1,2m+1}$ and $TM_{2n+1,2m+1}$ ($n=0, 1, 2, \cdots$,

Manuscript received January 24, 1967; revised April 4, 1967.

[1] B. M. Schiffmann and L. Young, "Design tables for an elliptic-function bandstop filter ($N=5$)," *IEEE Trans. Microwave Theory and Techniques*, vol. MTT-14, pp. 474–482, October 1966.

[2] H. Ozaki and J. Ishii, "Synthesis of transmission-line networks and the design of UHF filter," *IRE Trans. Circuit Theory*, vol. CT-2, pp. 325–336, December 1955.

[3] M. Soldi, "Solution of the approximation problem for distributed constant filters by means of Darlington reference filters," *Alta Frequenza*, vol. 34, pp. 340–348, May 1965.